Supporting Material

How Cations Change Peptide Structure

Dr. Carsten Baldauf,[*,†] Dr. Kevin Pagel,[*,†] Dipl.-Phys. Stephan Warnke,[†] Dr. Gert von Helden,[†] Prof. Dr. Beate Koksch,[‡] Dr. Volker Blum,[*,†] and Prof. Dr. Matthias Scheffler[†]

Fritz-Haber-Institut der Max-Planck-Gesellschaft, Faradayweg 4-6, D-14195 Berlin-Dahlem, Germany, and Institut für Chemie und Biochemie - Organische Chemie, Freie Universität Berlin, Takustr. 3, D-14195 Berlin-Dahlem, Germany

E-mail: baldauf@fhi-berlin.mpg.de; pagel@fhi-berlin.mpg.de; blum@fhi-berlin.mpg.de

Simulation details

Potential-energy surface scan

The potential-energy surface of the peptides AAPA and ADPA alone and in the presence of Li^+ or Na^+ is scanned for minima by a basin-hopping algorithm available from the TINKER 5 software tools for molecular design.[1–4] The underlying potential-energy surface (PES) is described by classical molecular mechanics, employing the protein force fields OPLS-AA[5] and AMBER (parm99,[6] with alkali metal parameters from reference 7). The TINKER 5 scan routine was parallelized in-house.[8] The PES-scan starts from a minimum and projects along *n* torsional normal

*To whom correspondence should be addressed
†Fritz-Haber-Institut der MPG
‡Freie Universität Berlin

modes to generate a new starting geometry for local optimization. This process is repeated until no new minima are found. Minima within a range ΔE relative to the current lowest energy found are accepted. Minima are considered identical if their energies agree with an accuracy x. The scan was first performed with loose criteria (n= 10, ΔE= 25 kcal/mol, x= 0.0001 kcal/mol/Å) and repeated starting from the found global minimum with tighter settings (n = 15, ΔE= 20 kcal/mol, x= 0.00001 kcal/mol/Å). The resulting conformations were clustered by a k-means clustering as provided in the MMTSB [9] with a radius of 0.7 to 1 Å of the Voronoi cells, resulting in 700 to 1,800 structures.

Density-functional theory

In order to describe the subtleties of the peptide structure formation and the impact of cation adsorption, we employ density-functional theory (DFT) in the generalized gradient approximation by means of the Perdew-Burke-Ernzerhof (PBE) functional.[10,11] In order to add description of the dispersion effects (van der Waals-type interactions) the Tkatchenko-Scheffler formalism is applied.[12] These methods are incorporated in the FHI-aims code for *ab initio* molecular simulation.[13] FHI-aims uses numeric atom-centered orbitals; accuracy and computational effort is tweaked by so-called species-defaults. For relaxing the thousands of conformations resulting from the preceding force field PES-scans, "*light*" species defaults (*tier-1*) were used.[13] For the relaxations of resulting conformers within a threshold of 35 kJ/mol above the lowest-energy structure and for all subsequent calculations "*tight*" species defaults (*tier-2*) were employed.[13] Vibrational frequencies of the systems were computed in the harmonic approximation via a finite differences approach. This allows for: (*i*) characterization of the stationary points as minima; (*ii*) computation of zero-point corrections and of harmonic free-energies at finite temperature; (*iii*) calculation of harmonic IR spectra.

Molecular dynamics simulations and theoretical infrared spectroscopy

Ab initio Born-Oppenheimer molecular dynamics (AIMD) simulations of the systems in the gas phase were performed for 10 ps at a constant temperature of 300 K (Nosé-Hoover thermostat[14,15]) for equilibration and then at constant energy for 20 to 40 ps to derive vibrational spectra from the development of the dipole moment over time.[16,17] The AIMD simulations were performed with an integration step size of 1 fs. Experimental and theoretical spectra were smoothed and subsequently splined with a step width of 0.5 cm^{-1} in the range from 1000 to 1800 cm^{-1}. Intensities were normalized to 1. For a quantitative comparison between the calculated and experimental spectra, we employ the reliability factor R_P introduced by Pendry[18] to the field of low-energy electron diffraction (LEED), in an implementation distributed with reference 19.

CCSD(T) extrapolation to the complete basis-set limit

Automatic basis-set extrapolation was performed as implemented in the ORCA software.[20] The method suggested by Truhlar was used.[21] Exchange and correlation energies are supposed to converge as follows:

$E_{ex}^{(X)} = E_{ex}^{(\infty)} + A\,exp(-\alpha\sqrt{X})$, $E_{corr}^{(\infty)} = \frac{X^\beta E_{corr}^{(X)} - Y^\beta E_{corr}^{(Y)}}{X^\beta - Y^\beta}$.

X and Y are the cardinal numbers of the Dunning basis sets cc-pVDZ ($X = 2$) and cc-pVTZ ($Y = 3$). For such a 2/3 extrapolation values of $\alpha = 4.42$ and $\beta = 2.4$ are suggested in the ORCA manual.[22]

Results

Protein force fields and DFT for AAPA + Li^+

The funnel-like shape of the FF results (if sorted according to their energy) and the dramatic scatter of the respective PBE+vdW results is illustrated in Figure 1. For a more detailed analysis we computed for PBE+vdW low energy conformers of AAPA+Li^+, potential energies employing the

hybrid density functional PBE0+vdW,[23] the polarizable force field (FF) Amoeba,[4] and for the classical protein FF Amber99,[24] Charmm22,[25] and OPLS.[5] The calculations (single point) were repeated for the same AAPA conformers (fixed geometries) but without the cation. The relative energies and mean absolute errors (MAE, $MAE = \frac{1}{n}\sum_{i=1}^{n}|f_i - y_i|$) are summarized in Table 1 and Table 2. While the MAE between the two DFT techniques is small ($\sim$1 kJ/mol), this value is contrasted by the results with different FF approaches (see Table 1 and Figure 2 in the main text), where the MAE's are consistently *much* larger, with significant errors also for the predicted conformational energy hierarchies. In short, even in the face of the relatively small discrepancies between PBE+vdW conformational energy hierarchies and the roughly estimated IR abundances, DFT based approaches for cation-peptide systems appear to be vastly preferable over FF-based approaches. Interestingly, the removal of the cation leads to still large MAE values, but the trend of the energy hierarchies appears more consistent between the methods.

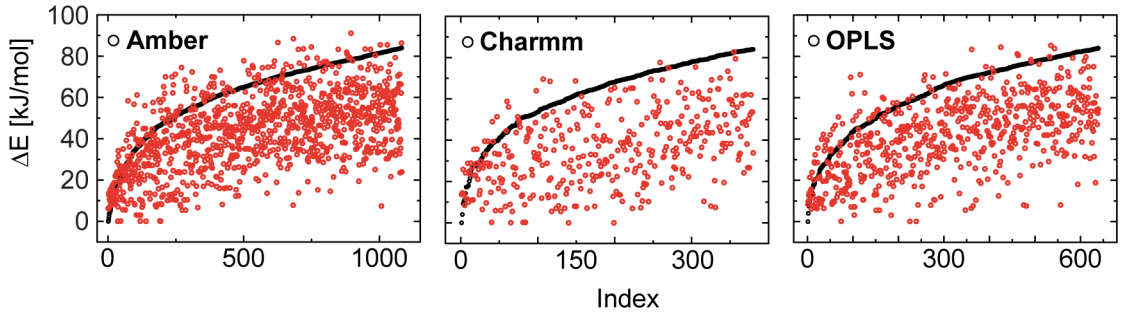

Figure 1: The conformations found in the FF PES scan can be sorted according to their energy, the lowest energy structure gets index 1, the second stable conformer index 2, and so on. Plotting relative energy versus index results in curves with a steep ascend for low index numbers which flattens towards higher index numbers (black circles). Relaxations of the respective conformers using DFT (PBE+vdW, "*light*" species defaults) and again plotting these energies against the original index number (red circles) indicates a serious scatter relative to the FF funnels.

Low-energy conformers of AAPA in isolation and in the presence of Li^+ or Na^+

Table 3 gives backbone conformations by means of the central backbone torsion angles ϕ and ψ of residues 2 and 3 of peptide AAPA. Furthermore, the table contains relative potential and free

Table 1: Relative potential energies (in kJ/mol) of AAPA + Li^+ conformers at the PBE+vdW, PBE0+vdW,[23] PBE, PBE0, Amoeba,[4] Amber99,[6] Charmm22,[25] and OPLS[5] level of theory and the mean absolute error (MAE) relative to PBE+vdW.

	Relative energies							
Conf.	PBE+vdW	PBE0+vdW	PBE	PBE0	Amoeba	Amber	Charmm	OPLS
1081	0.0	0.0	0.0	0.0	0.0	0.0	0.0	0.0
580	0.2	0.0	-2.3	-1.9	-8.9	-28.6	-42.8	-35.0
322	3.3	3.5	-0.8	-0.6	18.2	0.1	8.7	-2.5
138	3.8	2.0	-15.5	-15.8	22.1	3.3	1.8	-8.8
014	3.8	1.9	-11.8	-12.8	-1.6	-19.2	-34.1	-58.9
001	4.7	2.8	-9.6	-10.5	-17.7	-36.3	-44.7	-52.5
391	5.7	5.7	0.2	1.2	-3.9	-15.9	-30.0	-17.4
004	6.8	5.9	-6.2	-6.1	-9.7	-32.3	-32.5	-54.0
697	6.9	4.9	-7.0	-8.3	4.9	-16.1	-29.5	-55.2
396	6.9	6.3	-6.5	-6.5	9.5	-15.1	-21.7	-61.2
462	7.3	8.1	-4.5	-2.2	-3.2	17.5	-11.8	-12.5
646	7.5	5.3	-10.5	-11.2	29.1	8.4	6.6	-8.9
955	7.7	8.3	8.7	9.1	6.3	17.3	11.3	19.3
050	8.1	7.5	0.3	0.2	10.2	0.7	3.2	-7.1
417	8.4	7.0	-5.4	-5.8	-10.9	-35.4	-46.2	-56.6
745	8.5	8.8	7.6	8.3	-3.4	-12.6	-33.3	-17.1
324	8.5	9.1	-1.7	-0.3	11.1	-33.6	-69.8	-94.0
060	8.8	6.9	-9.9	-10.4	18.9	24.4	0.2	-7.6
798	9.3	10.7	2.1	4.4	15.3	-3.3	-32.2	-51.5
006	9.4	9.5	6.7	7.1	15.5	16.4	15.4	16.6
031	9.7	7.8	-6.9	-7.2	19.9	-10.0	-1.7	-2.2
MAE to PBE+vdW		1.0	10.0	9.9	9.6	18.7	26.1	35.2

Table 2: Relative potential energies (in kJ/mol) of AAPA + Li^+ conformers without the Li^+ cation at the PBE+vdW, PBE0+vdW,[23] Amoeba,[4] Amber99,[6] Charmm22,[25] and OPLS[5] level of theory and the mean absolute error (MAE) relative to PBE+vdW.

	Relative energies							
Conf.	PBE+vdW	PBE0+vdW	PBE	PBE0	Amoeba	Amber	Charmm	OPLS
1081	24.7	25.2	32.0	31.4	15.0	36.2	64.1	61.6
580	17.8	19.3	28.7	28.9	12.4	1.7	17.2	19.2
322	36.6	36.9	39.1	38.3	34.9	55.6	92.1	72.3
138	40.3	38.8	29.1	28.0	33.2	45.2	70.5	50.0
014	75.1	76.6	67.1	68.6	49.9	109.7	120.1	86.6
001	64.2	64.8	57.4	58.1	32.4	77.7	94.6	79.0
391	24.8	26.8	33.3	34.4	20.0	15.7	31.5	38.4
004	75.1	76.7	69.0	70.5	51.7	107.0	129.1	97.7
697	78.2	79.5	71.7	72.9	58.3	114.9	126.2	92.1
396	85.1	87.6	78.6	80.9	69.0	137.4	153.1	103.0
462	0.0	0.0	0.0	0.0	0.0	0.0	0.0	0.0
646	42.2	40.2	32.2	30.5	39.6	47.4	72.1	47.2
955	33.7	35.0	42.6	42.6	24.2	49.2	69.8	77.0
050	46.2	45.9	45.2	44.3	32.5	67.3	98.3	76.8
417	69.0	70.1	62.7	63.8	41.0	84.9	97.5	79.8
745	27.7	30.0	40.7	41.5	21.3	14.3	22.2	34.2
324	56.4	59.1	54.8	57.2	52.8	89.7	74.8	52.6
060	52.5	51.6	41.3	40.6	33.1	76.3	79.8	58.2
798	27.1	28.6	28.3	29.4	28.8	47.9	47.7	23.8
006	37.2	37.8	41.8	41.8	30.9	56.9	84.0	82.6
031	36.5	34.3	27.4	25.7	28.1	26.3	60.5	50.0
MAE to PBE+vdW		1.3	6.7	6.7	11.6	19.5	31.8	16.5

energies at the PBE+vdW and PBE0+vdW level of theory. PBE0+vdW values stem from single point calculations on PBE+vdW geometries; ΔF_{300K} at the PBE0+vdW level is the PBE0+vdW potential energy with a PBE+vdW harmonic free energy correction. Coordinates in xyz format are given for the conformers depicted in Figure 2 of the main text. For further structures contact Carsten Baldauf (baldauf@fhi-berlin.mpg.de).

The low free energy conformers of AAPA with either Li^+ or Na^+ were subject to AIMD simulations. Interestingly, conformer A1661 was not stable and the conformation changed to a $\beta II'$-turn, a significantly less stable conformer (see Figure 2). As a rough guide for the likelihood of the presence of a particular conformer in the postulated conformational ensemble, the R_P can serve. Figure 2 compares IR spectra of both conformers under discussion (0-1-2-4_A and $\beta II'$) with the experimental IR spectrum. None of the two shows a noteworthy agreement to experiment.

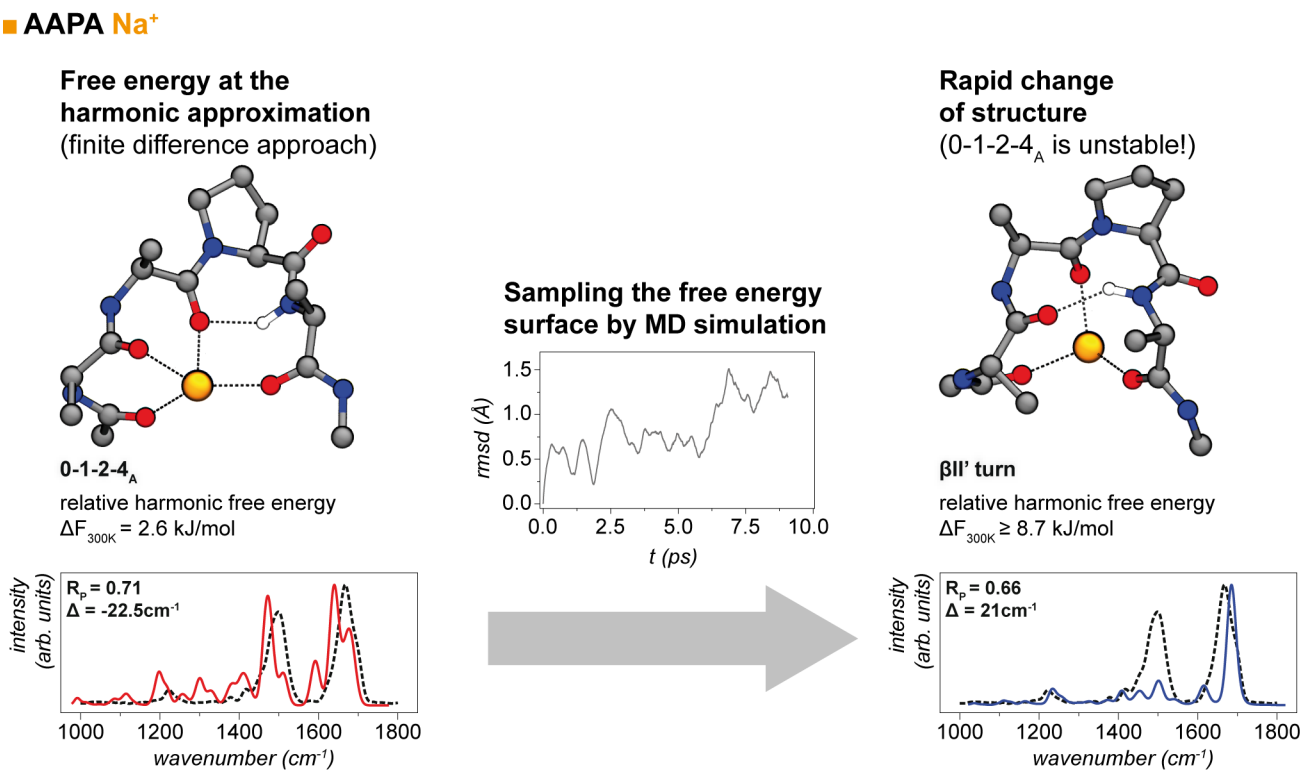

Figure 2: The conformer 0-1-2-4_A is a minimum at the potential energy surface and, considering harmonic free energy contributions, is one of the most stable structures for AAPA + Na^+. However, by sampling the free energy surface by means of AIMD simulations, the structure changes to a $\beta II'$ turn that is less stable in terms of harmonic free energy at 300 K. None of of the two conformers shows agreement with experimental IR spectra.

Low-energy conformers of ADPA in isolation and in the presence of Li^+ or Na^+

Table 4 gives backbone conformations by means of the central backbone torsion angles ϕ and ψ of residues 2 and 3 of peptide ADPA. Furthermore, the table contains relative potential and free energies at the PBE+vdW and PBE0+vdW level of theory. PBE0+vdW values stem from single point calculations on PBE+vdW geometries; ΔF_{300K} at the PBE0+vdW level is the PBE0+vdW potential energy with a PBE+vdW harmonic free energy correction. Coordinates in xyz format are given for the conformers depicted in Figure 3 of the main text. For further structures contact Carsten Baldauf (baldauf@fhi-berlin.mpg.de).

Table 3: Backbone torsion angles (in degree) of the central (turn-type defining) residues of AAPA in isolation and with Li^+ or Na^+. Relative potential (ΔE) and harmonic free energies (ΔF_{300K}) in kJ/mol. Conformer numbers in parentheses are for our internal bookkeeping.

	torsion angles					PBE+vdW		PBE0+vdW (SP)	
Conf.	ϕ_2	ψ_2	ω_3	ϕ_3	ψ_3	ΔE	ΔF_{300K}	ΔE	ΔF_{300K}
				AAPA					
$\beta VIa1$ (O001/A407)	-47.4	127.1	12.9	-82.0	-7.6	**0.0**	**0.0**	**0.0**	**0.0**
$\beta VIa1$ (O2790/A219)	-47.3	128.7	11.1	-73.3	-16.1	4.1	4.5	4.3	4.7
$\beta VIa2$ (A342)	-120.7	83.4	13.2	-108.0	11.4	7.9	8.3	9.5	9.9
$\beta II'$ (O063)	47.8	-114.7	-177.2	-64.8	-25.0	2.8	8.8	3.5	9.9
				AAPA+Li^+					
*0-2-4 (I) (138)	-54.6	154.3	175.9	-50.3	135.2	3.8	**0.0**	2.0	**0.0**
*0-1-2-4 (I) (001)	67.3	176.0	176.9	-63.5	-21.7	4.7	0.9	2.8	0.8
*0-1-2-4 (II) (014)	70.4	165.0	168.2	-56.1	136.4	3.8	2.2	2.0	2.2
*α-turn (580)	-58.6	-67.2	178.7	-64.0	-27.3	0.2	3.6	**0.0**	5.2
0-1-2-4 (III) (417)	69.0	167.3	175.5	-66.7	-17.0	8.4	3.6	7.1	4.1
0-2-4 (II) (031)	-55.9	160.8	179.9	-56.1	-29.7	9.7	4.3	7.8	4.1
0-2-4 (III) (646)	-52.7	153.3	176.6	-55.2	137.9	7.5	4.7	5.4	4.4
0-2-4 (IV) (060)	-58.8	156.3	176.7	-48.7	135.3	8.8	5.0	6.9	4.9
βVI (a2) (462)	-113.9	155.8	-1.5	-89.3	-5.0	7.3	5.3	8.1	7.8
βII' (322)	47.0	-132.2	-169.7	-71.3	-17.0	3.3	6.9	3.5	8.9
βII' (1081)	45.0	-126.7	-168.8	-71.4	-13.9	**0.0**	7.3	0.04	9.1
				AAPA+Na^+					
*0-1-3-4 (A120)	-108.8	150.0	-12.8	-58.6	156.2	6.5	**0.0**	6.4	**0.0**
#0-1-2-4_A (A1661)	77.9	157.1	176.2	-79.5	74.9	12.5	2.6	14.0	4.2
*0-1-2-4 (I) (O956-1)	70.6	175.7	177.7	-68.5	-18.0	9.3	3.9	7.5	2.3
*1-2-3-4 (A101)	-67.2	-51.6	176.5	-54.6	143.6	11.3	5.8	12.4	7.1
0-1-2-4 (III) (A179/O080)	72.3	164.5	176.9	-72.8	-13.1	11.7	6.8	10.3	5.5
$\beta VIa1$ (O016)	-71.4	163.2	-18.6	-68.0	-26.9	8.0	8.3	8.0	8.4
βII' (O590/A209)	49.1	-123.3	-172.7	-75.7	-10.2	**0.0**	8.7	**0.0**	8.8
α-turn (O808)	-66.4	-55.1	174.4	-64.7	-27.2	2.9	9.5	3.6	10.3
βVIb (A524)	-112.5	153.2	-10.6	-65.0	165.5	5.1	9.7	5.6	10.4
*0-1-2-4 (II) (O956-2)	77.0	157.5	168.7	-59.8	141.8	12.9	11.5	10.9	9.7

* ... considered for theoretical IR spectra

... unstable in subsequent *ab initio* molecular dynamics simulations

Table 4: Backbone torsion angles (in degree) of the central (turn-type defining) residues of ADPA in isolation and with Li^+ or Na^+. Relative potential (ΔE) and harmonic free energies (ΔF_{300K}) in kJ/mol. Conformer numbers in parentheses are for our internal bookkeeping.

	torsion angles					PBE+vdW		PBE0+vdW (SP)	
Conf.	ϕ_2	ψ_2	ω_3	ϕ_3	ψ_3	ΔE	ΔF_{300K}	ΔE	ΔF_{300K}
				ADPA					
SC-β (I) (005)	-170.2	172.3	-179.7	-57.0	-40.3	4.0	**0.0**	4.3	**0.0**
$\beta VIa1$ (I) (24777)	-38.0	117.1	15.5	-89.2	-3.1	0.7	2.0	0.8	1.8
$\beta VIa1$ (II) (11992)	-55.0	128.9	15.6	-82.9	-5.5	**0.0**	2.4	0.2	2.3
SC-β (II) (993)	-101.1	108.6	-177.6	-74.3	-24.3	2.0	2.5	**0.0**	0.1
SC-β (III) (6626)	-148.7	116.5	179.1	-76.3	-24.7	15.0	3.7	15.9	4.3
SC-β (IV) (081)	-99.3	106.9	-178.6	-65.3	-31.8	2.8	4.3	0.1	1.4
				ADPA+Li^+					
*0-2-4-SC (I) (620)	169.1	165.2	170.3	-57.2	137.3	3.9	**0.0**	5.4	**0.0**
*0-2-4-SC (II) (2580)	-51.5	156.4	163.4	-53.3	143.8	**0.0**	4.1	**0.0**	2.6
*0-2-4-SC (III) (421)	150.9	165.6	-176.8	-63.9	-23.4	7.0	4.9	8.7	5.1
*0-2-4-SC (IV) (123)	150.8	165.6	-176.8	-63.8	-23.5	7.0	5.4	8.9	5.6
0-2-4-SC (V) (831)	-70.2	162.6	165.9	-52.3	138.4	14.2	7.3	14.0	5.6
				ADPA+Na^+					
*0-2-4-SC (I) (321)	155.5	168.7	-177.6	-70.1	-16.9	**0.0**	**0.0**	0.1	0.6
*0-2-4-SC (II) (19043)	-64.2	164.3	166.7	-55.5	145.9	11.8	2.9	8.4	**0.0**
*0-2-4-SC (III) (3606)	106.7	166.1	-172.5	-82.3	-1.8	14.6	4.9	12.4	3.2
*0-2-4-SC (IV) (1082)	-54.9	149.0	-176.8	-57.1	-33.2	1.0	6.2	1.8	7.6
0-2-3-4 (2336)	73.1	169.0	175.6	-52.1	-49.8	7.6	11.7	9.1	13.7
1-2-4 (2529)	-50.5	148.3	157.4	-51.4	139.3	8.1	12.0	8.2	13.0

* ... considered for theoretical IR spectra

Notes and References

(1) Ponder, J.; Richards, F. *J Comput Chem* **1987**, *8*, 1016–1024.

(2) Pappu, R.; Hart, R.; Ponder, J. *J Phys Chem B* **1998**, *102*, 9725–9742.

(3) Ren, P.; Ponder, J. *J Phys Chem B* **2003**, *107*, 5933–5947.

(4) Schnieders, M.; Ponder, J. *J Chem Theory Comput* **2007**, *3*, 2083–2097.

(5) Jorgensen, W.; Ulmschneider, J.; Tirado-Rives, J. *J Phys Chem B* **2004**, *108*, 16264–16270.

(6) Wang, J.; Cieplak, P.; Kollman, P. *J Comput Chem* **2000**, *21*, 1049–1074.

(7) Ross, W.; Hardin, C. *J Am Chem Soc* **1994**, *116*, 6070–6080.

(8) Unpublished parallel version of the TINKER 5 scan routine by Sucismita Chutia (FHI Berlin).

(9) Feig, M.; Karanicolas, J.; Brooks III, C. *J Mol Graph Modell* **2004**, *22*, 377–395.

(10) Perdew, J. P.; Burke, K.; Ernzerhof, M. *Phys Rev Lett* **1996**, *77*, 3865–3868.

(11) Perdew, J. P.; Burke, K.; Ernzerhof, M. *Phys Rev Lett* **1997**, *78*, 1396–1396.

(12) Tkatchenko, A.; Scheffler, M. *Phys Rev Lett* **2009**, *102*, 73005.

(13) Blum, V.; Gehrke, R.; Hanke, F.; Havu, P.; Havu, V.; Ren, X.; Reuter, K.; Scheffler, M. *Comput Phys Commun* **2009**, *180*, 2175–2196.

(14) Hoover, W. G. *Phys Rev A* **1985**, *31*, 1695–1697.

(15) Nose, S. *J Chem Phys* **1984**, *81*, 511–519.

(16) Gaigeot, M.-P. *Phys Chem Chem Phys* **2010**, *12*, 3336–3359.

(17) Rossi, M.; Blum, V.; Kupser, P.; von Helden, G.; Bierau, F.; Pagel, K.; Meijer, G.; Scheffler, M. *J Phys Chem Lett* **2010**, *1*, 3465–3470.

(18) Pendry, J. *J Phys C: Solid State Phys* **1980**, *13*, 937–944.

(19) Blum, V.; Heinz, K. *Comput Phys Commun* **2001**, *134*, 392–425.

(20) Neese, F. *WIREs Comput Mol Sci* **2012**, *2*, 73–78.

(21) Truhlar, D. G. *Chem Phys Lett* **1998**, *294*, 45 – 48.

(22) Neese, F. *ORCA Manual Version 2.9*, 2012. `http://www.mpibac.mpg.de/bac/logins/neese/downloads/OrcaManual_2_9.pdf`.

(23) Adamo, C.; Barone, V. *J Chem Phys* **1999**, *110*, 6158–6170.

(24) Wang, J.; Cieplak, P.; Kollman, P. *J Comput Chem* **2000**, *21*, 1049–1074.

(25) MacKerell Jr., A. D. et al. *J Phys Chem B* **1998**, *102*, 3586–3616.